# SEAL: SEMANTIC-AUGMENTED IMITATION LEARNING VIA LANGUAGE MODEL

**Chengyang Gu**[*,†], **Yuxin Pan**[*], **Haotian Bai**[*], **Hui Xiong**[*], **Yize Chen**[§†]
The Hong Kong University of Science and Technology (Guangzhou)[*], University of Alberta[§]

## ABSTRACT

Hierarchical Imitation Learning (HIL) is effective for long-horizon decision-making, but it often requires extensive expert demonstrations and precise supervisory labels. In this work, we introduce SEAL, a novel framework that leverages the semantic and world knowledge embedded in Large Language Models (LLMs) to autonomously define sub-goal spaces and pre-label states with semantically meaningful sub-goal representations, without requiring prior task hierarchy knowledge. SEAL utilizes a dual-encoder architecture that combines LLM-guided supervised sub-goal learning with unsupervised Vector Quantization (VQ) to enhance the robustness of sub-goal representations. Additionally, SEAL incorporates a transition-augmented low-level planner, which improves adaptation to sub-goal transitions. Our experimental results demonstrate that SEAL outperforms state-of-the-art HIL and LLM-based planning approaches, particularly when working with small expert datasets and complex long-horizon tasks.

## 1 INTRODUCTION

The advancement of LLMs brings transformative change to how agents learn to interact and make decisions (Brohan et al., 2023; Wang et al., 2023). LLMs like GPT-4 (Achiam et al., 2023) possess remarkable semantic understanding ability (Liu et al., 2023), human-like reasoning capability (Wei et al., 2022), and rich common sense knowledge (Bubeck et al., 2023), enabling them extracting insights from language instructions to support decision-making agents (Eigner & Händler, 2024).

A popular paradigm for LLM-assisted decision-making is to enhance Deep Reinforcement Learning (DRL) agents through improved reward design (Kwon et al., 2023; Ma et al., 2023). However, DRL suffers from sample inefficiency, requiring extensive interactions with the environment, particularly for long-horizon tasks with sparse rewards (Zhang et al.). In contrast, Imitation Learning (IL) avoids the expensive exploration of DRL by learning generalizable policies from expert demonstrations (Schaal, 1996). Yet, IL struggles with compounding errors in long-horizon tasks, leading to significant trajectory deviations (Nair & Finn, 2019). To address this, *Hierarchical Imitation Learning (HIL)* (Le et al., 2018a) decomposes long-horizon tasks into a multi-level hierarchy of sub-goals, reducing the relevant state-action space for each sub-goal, such as goal-states (Ding et al., 2019) and task IDs (Kalashnikov et al., 2021). Recent works explore using more informative, flexible language instruction for sub-goal specification (Stepputtis et al., 2020). While these works have demonstrated impressive results (Prakash et al., 2021; Hejna et al., 2023), learning effective language-based sub-goals remains challenging due to the need for large, expensive expert-labeled datasets (Chevalier-Boisvert et al., 2018a). Although several methods have been proposed to address this issue by inferring sub-goal boundaries with supervision-free algorithms (Garg et al., 2022; Jiang et al., 2022; Kipf et al., 2019; Simeonov et al., 2021), the unstructured language instructions still limit generalization to new tasks and hinder seamless integration into IL policy training(Wang et al., 2019a; Mees et al., 2022).

The capabilities brought by Large Language Models (LLMs) offer a new promising solution to tackle the limitations of traditional HIL methods. LLMs' strong reasoning and semantic abilities have been shown to help break down complex, ambiguous language instructions into manageable steps for high-level planning (Huang et al., 2022; Ahn et al., 2022; Huang et al., 2023). Notably,

[†]Corresponding Authors: cgu893@connect.hkust-gz.edu.cn, yize.chen@ualberta.ca

LLMs excel at emulating human-like task decomposition (Huang et al., 2022; Wei et al., 2022), and researchers have already harnessed this capability to generate structured high-level plans based on textual task instructions (Ahn et al., 2022; Prakash et al., 2023; Huang et al., 2023). However, LLMs still face challenges in generating directly executable plans, as they rely on pre-trained low-level policy agents to perform primitive actions (Prakash et al., 2023). Additionally, most high-level plans remain static and require frequent, costly interactions with LLM APIs(Song et al., 2023; Hu et al., 2023). These issues limit the scalability of LLM-based approaches in HIL. Motivated by these promises and challenges, we aim to answer the following question: *"Can pre-trained LLMs serve as a prior for identifying task's hierarchical structure? How to autonomously establish sub-goal library and guide both high-level sub-goal learning and low-level agent?"*

In this paper, we answer such questions firmly, where we design a novel scheme to let LLM generate high-level plans to assist sub-goal learning and policy training jointly in Hierarchical Imitation Learning framework. The proposed ***SE**mantic-**A**ugmented Imitation **L**earning* **(SEAL)** uses LLMs to generate high-level sub-goals as one-hot vector representations, which serve as supervisory labels for learning a lightweight encoder. This reduces the need for continuous LLM APIs calling while retaining the hierarchical structure dictated by the LLM. Additionally, SEAL incorporates a dual-encoder design, combining LLM-based supervised sub-goal learning with an unsupervised Vector Quantization (VQ) encoder (Wang et al., 2019b), which maps expert demonstrations to latent sub-goals. The dual-encoder structure enhances robustness and reduces overfitting by mitigating reliance on weaker encoders (evaluated by their contribution to action selection with success rate as the metric). To further improve sub-goal completion, SEAL employs a transition-augmented low-level policy, which implicitly prioritizes intermediate states corresponding to sub-goal transitions. Experiments on the *KeyDoor* and *Grid-World* tasks show that SEAL outperforms several state-of-the-art HIL approaches. To summarize, our main contributions include:

- We propose SEAL, a novel HIL framework that leverages LLMs to autonomously generate high-level plans and sub-goal representations without prior hierarchical knowledge.
- To enhance SEAL's effectiveness, we introduce: (1) A dual-encoder structure combining supervised LLM-based sub-goal learning and unsupervised VQ-based representations for robust sub-goal learning (2) A transition-augmented low-level planner that improves handling of intermediate states and sub-goal transitions.
- Extensive experiments showSEAL's superior performance against several state-of-the-art HIL approaches, in small datasets, long-range tasks, and task variations.

## 2 Related Works

**Imitation Learning.** Imitation Learning encompasses two primary approaches: Behavioral Cloning (BC) (Bain & Sammut, 1995) and Inverse Reinforcement Learning (IRL) (Ng et al., 2000). BC relies on a pre-collected expert dataset of demonstrations, where the agent learns to mimic the actions in an offline manner. While BC is simple to implement, it is prone to compounding errors, particularly when the agent encounters states not present in the expert's demonstrations (Zhang, 2021). In contrast, IRL methods (Ho & Ermon, 2016; Reddy et al., 2019; Brantley et al., 2019) involve interacting with the environment to collect additional demonstrations, aiming to infer the underlying reward function that the expert is optimizing. The agent then learns by optimizing this inferred reward. However, IRL approaches are more challenging to implement (Kurach et al., 2018), typically requiring more computational resources and data. In this work, we primarily adopt the BC architecture in a hierarchical setting, while incorporating insights from IRL by using environment interactions to validate the reliability of learned latent sub-goal variables.

**Bi-Level Planning and Execution.** Hierarchical Imitation Learning (HIL) enhances the ability of imitation learning agents to tackle complex, long-horizon tasks by breaking them down into smaller sub-goals and conditioning the agent's behavior on those sub-goals. The high-level agent chooses the sub-goals, while the low-level agent learns to accomplish specific controls under selected sub-goals (Jing et al., 2021). Many HIL approaches, such as Hierarchical Behavior Cloning (Le et al., 2018a) and Thought Cloning (Hu & Clune, 2024), rely on supervisory labels for sub-goal learning, but such annotations are often difficult to obtain. To address this limitation, unsupervised methods like Option-GAIL (Jing et al., 2021), LOVE (Jiang et al., 2022), SDIL (Zhao et al., 2023), and CompILE (Kipf et al., 2019) have been developed to infer sub-goals directly from expert trajectories.

However, the lack of labeled guidance in these approaches makes meaningful sub-goal discovery more challenging and hence reduces the reliability of the learned policies.

**LLMs for Planning.** Large Language Models (LLMs) have demonstrated significant potential in decision-making processes. Direct generation of action sequences usually do not lead to accurate plans (Silver et al., 2022; Valmeekam et al., 2023; Kambhampati et al., 2024). Recent studies have successfully utilized LLMs to decompose natural language task instructions into executable high-level plans, represented as a sequence of intermediate sub-goals (Ahn et al., 2022; Prakash et al., 2023; Huang et al., 2023). While LLMs can be also applied to translate user-given language instructions to symbolic goals (Mavrogiannis et al., 2024; Xie et al., 2023) Additionally, LLMs can function as encoders, identifying current sub-goals based on both observations (sometimes images) and language task descriptions to facilitate high-level plan execution (Fu et al., 2024; Malato et al., 2024; Du et al., 2023). However, these approaches typically still depend on pre-trained low-level planners for generating executable primitive actions. In this work, we leverage LLM-generated high-level plans to assist in learning both sub-goals and low-level actions simultaneously.

## 3 PRELIMINARY

In this paper, we look into the long-horizon, compositional decision-making problem as as a discrete-time, finite-step **Markov Decision Process (MDP)**. MDP can be represented by a tuple $(\mathcal{S}, \mathcal{A}, \mathcal{T}, r, \gamma)$, where $\mathcal{S}$, $\mathcal{A}$ denotes the state and action space, $\mathcal{T}(s_{t+1}|s_t, a_t) : \mathcal{S} \times \mathcal{A} \to \mathcal{S}$ denotes the transition function, $r : \mathcal{S} \times \mathcal{A} \to \mathbb{R}$ is the reward function and $\gamma \in [0, 1]$ is the discount factor.

In standard settings of Hierarchical Imitation Learning (HIL), instead of having access to the reward function $r$, the agent has access to a dataset of expert demonstrations $\mathcal{D} = \{\tau_1^e, \tau_2^e, ..., \tau_N^e\}$, which contains $N$ expert trajectory sequences consisting of state-action pairs $\{(s_t, a_t)\}$, where $s_t \in \mathcal{S}$, $a_t \in \mathcal{A}$, $T$ is the time horizon for planning, $0 \leq t \leq T$. In this paper, the expert trajectories are not labeled with any rewards nor subhorizon segments. We assume HIL agents operate in a two-level hierarchy though our method can also be applied to problems with more levels:

- **High-level Sub-goal Encoder** $\pi_H(g_t|s_t)$: Selects a sub-goal $g_t \in \mathcal{G}$ based on the current states $s_t$, where $\mathcal{G}$ is the space of sub-goals.
- **Low-level Policy Agent** $\pi_L(a_t|g_t, s_t)$: Executes actions conditioned on both the current state $s_t$ and sub-goal $g_t$.

In this work, we focus on settings where agents lack access to the sub-goal space $\mathcal{G}$, relying instead on an oracle full task instruction $\mathcal{M}$ in natural language. While well-defined $\mathcal{G}$ aids efficient HIL agent learning (Hauskrecht et al., 2013), its acquisition is difficult due to missing task-specific knowledge (Nachum et al., 2018; Kim et al., 2021). Natural language task instructions, though easier to obtain as they are common-used commands from human (Stepputtis et al., 2020), are hard to map to hierarchical structures due to their complex and ambiguous nature (Zhang & Chai, 2021; Ahuja et al., 2023; Ju et al., 2024). In this work, we investigate leveraging LLMs to parameterize $\mathcal{G}$ from language instructions with its powerful semantic and world knowledge, and pre-label states in $\mathcal{D}$ to guide effective learning of $\pi_H$ and $\pi_L$ in hierarchical imitation learning.

## 4 SEAL FOR HIERARCHICAL IMITATION LEARNING

The key idea of SEAL is to learn high-level sub-goal representations using supervisory labels generated by LLMs. In previous works, such labels were typically provided by human experts via instructions (Pan et al., 2018; Le et al., 2018a), making them expensive to obtain. However, with the assistance of LLMs, we introduce an efficient and reliable method to automatically generate labels that map states to sub-goals. Specifically, LLMs are used to semantically extract a high-level plan from the full-task language instruction $\mathcal{M}$ and map states in expert demonstrations to sub-goals within this plan. Using these learned sub-goal representations, the model then learns the corresponding low-level actions. An overview of our SEAL framework is illustrated in Fig. 1.

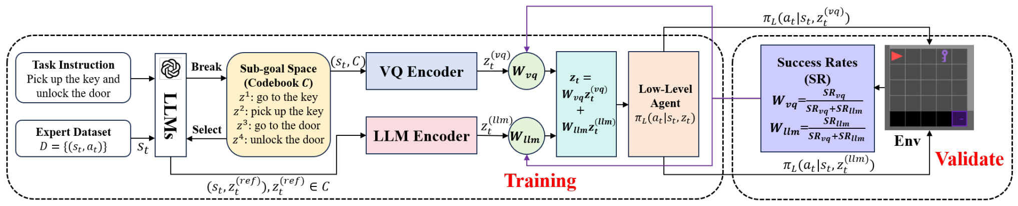

Figure 1: **Overview of SEAL Architecture:** The LLM aids in discovering sub-goal spaces for the task by semantically decomposing the full-task instruction and labeling each state with a reference latent vector that represents its corresponding sub-goal. These reference labels are then used to train a high-level sub-goal encoder, which works in conjunction with an unsupervised VQ encoder.

## 4.1 Pretrained LLMs for Guiding Sub-Goals Learning

Our key design of leveraging LLMs to guide high-level sub-goals learning can be divided into two stages: (i) Use LLM-generated high-level plan based on full-task instruction as **sub-goal space**; (ii) Let LLMs encode states in expert demonstrations to sub-goal representations.

**Derive Sub-goal Space of Task** Prior works have demonstrated that LLMs can establish a meaningful chain of sub-tasks from task instruction as high-level plan (Huang et al. (2022); Prakash et al. (2023); Singh et al. (2023)). Yet few of them incorporate it with Hierarchical Imitation Learning (HIL). In SEAL, we use LLMs to specify the unknown sub-goal space $\mathcal{G}$ in HIL formulations. Feeding LLMs with the full-task language instruction $\mathcal{M}$, we notice that the decomposed sub-goals in high-level plan naturally consist of a language-based sub-goal set: $\{\hat{g}^1, \hat{g}^2, ..., \hat{g}^K\} = f_{llm}(\mathcal{M})$, where $K$ is the total number of generated sub-goals. We treat this estimated sub-goal dataset as the finite sub-goal space: $\mathcal{G} = \{\hat{g}^1, \hat{g}^2, ..., \hat{g}^K\}$.

**Labeling Sub-goals for States in Expert Dataset** After devising the sub-goal space $\mathcal{G}$ with LLM-generated sub-goals, we use them to map states $s_t \in \mathcal{D}$ to a sub-goal latent space. These LLM-defined labels guide the high-level encoder to learn task-relevant sub-goal representations. To parameterize the language-based sub-goals $\hat{g}^i \in \mathcal{G}$ and facilitate learning, we establish a codebook $\mathcal{C} = \{z^1, z^2, ..., z^K\}$, where each latent variable $z^i \in \mathbb{R}^K$ is a one-hot vector (*i.e.* $i$-th element in $z^i$ equals to 1, others equal to 0, $i = 1, 2, ..., K$) representing sub-goal $\hat{g}^i$ in $\mathcal{G}$. We then prompt the same LLM to perform a encoding function $h_{llm}$, which map $s_t$ to latent vector $z_t^{(ref)} \in \mathcal{C}$ by checking whether it belongs to sub-goal $\hat{g}^i \in \mathcal{G}$: $z_t^{(ref)} = h_{llm}(s_t, \mathcal{G})$. We stipulate the output of LLM must be 'yes' or 'no' and then convert it to integer 1 or 0, as this form of answer has shown to be more reliable than the open-ended answer (Du et al. (2023)). By repeatedly asking $K$ times we can finally establish the $K$-dim latent variable $z_t^{(ref)}$ which represents the sub-goal for all $s_t$ in $\mathcal{D}$. We use these LLM-given latent representations $z_t^{(ref)}$ as supervisory labels for high-level sub-goal encoder training in HIL. Once we obtain these labels, we have no need to interact to LLMs later.

## 4.2 Dual-Encoder for Sub-goal Identification

Naturally, we consider using these LLM-generated labels for sub-goal representations to train a high-level sub-goal encoder $\pi_H(s_t)$ in a supervised manner. Compared to previous unsupervised approaches, this supervised method helps reduce the randomness of output sub-goals by leveraging the guidance provided by the labels. However, it is prone to over-fitting on the training dataset. To address this challenge, inspired by (Ranzato & Szummer (2008); Le et al. (2018b)), we propose a *Dual-Encoder* structure for high-level sub-goal identification. This design integrates both a supervised learning encoder and an unsupervised learning encoder, producing a weighted-average sub-goal representation. The weighted combination allows for flexibility, prioritizing the encoder that performs better for a particular task or dataset, ultimately enhancing robustness and improving generalization.

**Supervised LLM-Label-based Encoder** Considering that the codebook $\mathcal{C}$, representing the sub-goal space $\mathcal{G}$, is discrete and finite, we formulate the supervised sub-goal learning as a multi-class classification problem. To train this supervised learning encoder $\pi_H^{(llm)}$, we define the sub-goal learning objective by maximizing the log-likelihood of the labels generated by the LLMs:

$$\mathcal{L}_H^{(llm)} = \mathbb{E}_{(s_t, z_t^{(ref)})\sim\mathcal{D}} \; - \log \pi_H^{(llm)}(z_t^{(ref)}|s_t). \tag{1}$$

**Unsupervised VQ Encoder** Given the codebook $\mathcal{C} = \{z^1, z^2, ..., z^K\}$, we apply Vector Quantization (VQ) (Van Den Oord et al. (2017)) to design the unsupervised sub-goal encoder in our SEAL framework. It is a widely used approach that can map the input state $s_t$ to a finite, discrete latent space like $\mathcal{C}$. In VQ, the encoder $\pi_H^{(vq)}$ first predicts a continuous latent vector: $z_t^{(con)} = \pi_H^{(vq)}(s_t)$. This latent vector is then matched to the closest entry in $\mathcal{C}$:

$$z_t^{(vq)} = \text{argmin}_{z^i\in\mathcal{C}} \quad \|z_t^{(con)} - z^i\|_2^2. \tag{2}$$

The learning objective of $\pi_H^{(vq)}$, named *commitment loss*, encourages the predicted continuous latent vector $z_t^{(con)}$ to cluster to the final output sub-goal representation $z_t^{(vq)}$:

$$\mathcal{L}_H^{(vq)} = \mathbb{E}_{(s_t)\sim\mathcal{D}} \quad \|\text{stop\_gradient}(z_t^{(vq)}) - z_t^{(con)}\|_2^2; \tag{3}$$

where stop_gradient$(\cdot)$ denotes stop-gradient operation.

### 4.3 Transition-Augmented Low-level Policy

We compute a weighted-average vector $z_t$ over $z_t^{(llm)}$,$z_t^{(vq)}$ obtained by dual-encoders to finalize the predicted sub-goal representation:

$$z_t = W_{vq} z_t^{(vq)} + W_{llm} z_t^{(llm)}; \tag{4}$$

where the weights $W_{vq}$ and $W_{llm}$ quantifies *how the predicted sub-goal representations $z_t^{(vq)}$ and $z_t^{(llm)}$ contribute to the task completion success rate.* The weights are updated by validations during the training process. The update details will be demonstrated in Section 4.4.

Given the predicted sub-goal representations $z_t$ for each $s_t$ in the expert dataset, normally the low-level policy agent follows a goal-conditioned behavioral cloning (GC-BC) architecture. It is trained by maximizing the log-likelihood of the actions in the expert dataset, using the sub-goal representations as auxiliary inputs:

$$\mathcal{L}_{GC-BC} = \mathbb{E}_{(s_t, a_t, z_t)\sim\mathcal{D}} \; - \log \pi_L(a_t|s_t, z_t). \tag{5}$$

However, this low-level policy design overlooks the imbalanced distribution and importance of the hierarchical structure captured by high-level sub-goal encoders. Several studies have highlighted that certain states, where transitions between sub-goals occur in long-horizon demonstrations, have a significant impact on the policy agent's performance (Jain & Unhelkar, 2024; Zhai et al., 2022; Wen et al., 2020). Despite their critical role, these states make up only a small portion of expert demonstrations. Successfully reaching these intermediate states and taking appropriate actions improves sub-goal completion, thereby increasing the overall task success rate. We formally define these states as *intermediate states*:

**Definition 4.3.1. (Intermediate States).** Let $s_t \in \mathcal{S}, 0 \leq t \leq T$ be a state observed when running the HIL agent, $z_t$ is its corresponding latent variable learnt by high-level encoder $\pi_H$ that represents sub-goal. $s_{t+1}$ is the following state. The state $s_t$ is defined as an *intermediate state* only when the sub-goal changes: $z_{t+1} \neq z_t$.

Due to the scarcity of these intermediate states, it becomes very challenging to imitate the correct behavior in such states. To address this issue, inspired by the practice of assigning extra rewards to sub-goal transition points in hierarchical RL (Ye et al. (2020); Berner et al. (2019); Zhai et al. (2022); Wen et al. (2020)), we augment the importance of these intermediate states by assigning higher weights to them in the low-level policy training loss:

$$\mathcal{L}_L = \mathbb{E}_{(s_t, a_t, z_t)\sim\mathcal{D}} \; - e^{\|z_{t+1} - z_t\|_2^2} \log \pi_L(a_t|s_t, z_t); \tag{6}$$

where the term $e^{\|z_{t+1} - z_t\|_2^2}$ measures the L2-distance between the current sub-goal representation $z_t$ and the next sub-goal $z_{t+1}$. Given that $z_t$ is a one-hot vector, we have the term:

$$e^{\|z_{t+1} - z_t\|_2^2} = \begin{cases} e, \text{ if } z_{t+1} \neq z_t \\ 1, \text{ if } z_{t+1} = z_t \end{cases} \tag{7}$$

Thus, this term can serve as an adaptive weight to enhance the imitation of expert behavior at intermediate states. By incorporating this transition-augmented low-level policy design, we emphasize the importance of sub-goal transitions, and in simulations we also observe this design can greatly help agents make transitions across each sub-goal.

### 4.4 TRAINING

We train our SEAL model end-to-end, jointly updating parameters of $\pi_H$ and $\pi_L$ by minimizing the loss function $\mathcal{L} = \beta\mathcal{L}_H + \mathcal{L}_L$, where $\beta$ is a hyper-parameter that controls the weight of high-level sub-goal learning in relation to the overall training process. Additionally, in order to evaluate the reliability of the latent variables predicted by the VQ encoder and LLM-Label-based encoder and determine the weight combination that can better improve task performance, we keep validating the success rates of those two different latent variables in the environment during training. Based on the validation results, we dynamically update the weights $W_{vq}$ and $W_{llm}$ in Eq. 4.

For validation, we simultaneously execute actions conditioned on both the VQ-encoder and the LLM-label-based encoder: $a_t^{(vq)} = \pi_L(s_t, z_t^{(vq)})$ and $a_t^{(llm)} = \pi_L(s_t, z_t^{(llm)})$. We then *run episodes to test the different success rates*, $SR_{vq}$ and $SR_{llm}$, for completing the full task. The updated weights $W_{vq}$ and $W_{llm}$ are then computed as $W_{vq} = SR_{vq}/(SR_{llm} + SR_{vq})$; $W_{llm} = SR_{llm}/(SR_{llm} + SR_{vq})$ respectively. $W_{vq}$, $W_{llm}$ measure the relative task-completion performance of the policy agent under the guidance of $z_t^{(vq)}$ and $z_t^{(llm)}$, respectively. We refer to these weights as *confidences*, indicating the preference for trust between $z_t^{(vq)}$ and $z_t^{(llm)}$.

We also use these weights to finalize the overall training loss of SEAL as a weighted combination of two end-to-end losses under guidance $z_t^{(llm)}$ and $z_t^{(vq)}$. We finalize the overall training loss of SEAL by using a weighted combination of two end-to-end losses, conditioned on $z_t^{(llm)}$ and $z_t^{(vq)}$, with the same weights $W_{vq}$, $W_{llm}$ determining the contribution of each loss:

$$\mathcal{L}_{vq} = \beta\mathcal{L}_H^{(vq)}(s_t) + \mathcal{L}_L(s_t, z_t^{(vq)}); \mathcal{L}_{llm} = \beta\mathcal{L}_H^{(llm)}(s_t) + \mathcal{L}_L(s_t, z_t^{(llm)}); \mathcal{L}_{SEAL} = W_{vq}\mathcal{L}_{vq} + W_{llm}\mathcal{L}_{llm}. \tag{8}$$

Since the low-level policy agent's actions are conditioned on the latent sub-goal representations, minimizing this weighted-combination loss $\mathcal{L}_{SEAL}$ allows our SEAL to adapt the trainable parameters of the low-level policy based on task-completion performance. This approach helps the agent make better decisions by adjusting to updated latent predictions $z_t = W_{vq}z_t^{(vq)} + W_{llm}z_t^{(llm)}$ during training process. As a result, our SEAL framework can continuously adapt both the high-level sub-goal encoders and the low-level policy agent, leading to more reliable and robust sub-goal representations, as well as improved decision-making for action selection. The complete algorithm for SEAL is illustrated in Algorithm 1.

## 5 EXPERIMENTS

In this section, we evaluate the performance of SEAL on two long-horizon compositional tasks: *KeyDoor* and *Grid-World* (See detailed settings in Appendix). We compare SEAL's performance with various baselines, including non-hierarchical, unsupervised, and supervised hierarchical IL methods, in both large and small expert dataset scenarios. Following this, we analyze how SEAL enhances task completion performance.

### 5.1 BASELINES

We compare SEAL with four other approaches: one non-hierarchical approach, Behavioral Cloning (BC) (Bain & Sammut, 1995), two unsupervised approaches, LISA (Garg et al., 2022) and SDIL (Zhao et al., 2023), and one LLM-enabled supervised approach, Thought Cloning (TC) (Hu & Clune, 2024). The details of each method are as follows:

**Behavioral Cloning (BC)**: A classical non-hierarchical imitation learning method, where the policy agent $\pi(a_t|s_t)$ is trained by maximizing the log-likelihood: $\mathcal{L}_{BC} = \mathbb{E}_{(s_t,a_t)\in\mathcal{D}} \quad -\log\pi(a_t|s_t)$.
**LISA**: A hierarchical imitation learning (HIL) approach with an unsupervised VQ-based sub-goal learner. We implement the low-level policy using only the current state $s_t$, rather than a sequence of

**Algorithm 1** SEmantic-Augmented Imitation Learning (SEAL) via Language Model

```
1:  **Input:** Expert Trajectory Dataset $\mathcal{D}$, Natural Language Task Instruction $\mathcal{M}$, Pre-trained LLM $llm$ for sub-goal decomposition and labeling.
2:  **Initialize** VQ-encoder $\pi_H^{(vq)}(s_t;\theta_1)$, LLM-Label-based encoder $\pi_H^{(llm)}(s_t;\theta_2)$, Low-level policy agent $\pi_L(s_t, z_t;\theta_3)$, $W_{vq} = W_{llm} = 0.5$ .
3:  (**LLM Guiding Sub-goal Learning**)
4:  Specify sub-goal space with $\mathcal{M}$: $\mathcal{G} = \{\hat{g}^1, \hat{g}^2, ..., \hat{g}^K\} = f_{llm}(\mathcal{M})$ .
5:  Labeling $s_t \in \mathcal{D}$ to latent sub-goal representations $z_t^{(ref)}$: $z_t^{(ref)} = h_{llm}(s_t, \mathcal{G})$ ($z_t^{(ref)} \in \mathcal{C} = \{z^1, z^2, ..., z^K\}$) .
6:  (**Training**)
7:  **for** Iteration $j$ ($j = 1, 2, ..., J_{max}$) **do**
8:      For $s_t \in \mathcal{D}$, $z_t^{(llm)} \leftarrow \pi_H^{(llm)}(s_t)$,   $z_t^{(vq)} \leftarrow \pi_H^{(vq)}(s_t)$.
9:      Get $\mathcal{L}_H^{(llm)}$ and $\mathcal{L}_H^{(vq)}$ using Eq. 1 and Eq. 3.
10:     $\mathcal{L}_L^{(llm)} \leftarrow \mathcal{L}_L(s_t, a_t, z_t^{(llm)}), \mathcal{L}_L^{(vq)} \leftarrow \mathcal{L}_L(s_t, a_t, z_t^{(vq)})$, using Eq. 6.
11:     $\mathcal{L}_{SEAL} \leftarrow W_{llm}(\mathcal{L}_H^{(llm)} + \mathcal{L}_L^{(llm)}) + W_{vq}(\mathcal{L}_H^{(vq)} + \mathcal{L}_L^{(vq)})$
12:     Update $\theta_1$, $\theta_2$, $\theta_3$: $\theta_i \leftarrow \theta_i - \frac{\partial \mathcal{L}_{SEAL}}{\partial \theta_i}$ ($i = 1, 2, 3$)
13:     Validate for: $SR_{(llm)}, SR_{(vq)}$
14:     Update: $W_{vq} = \frac{SR_{vq}}{SR_{llm} + SR_{vq}}, W_{llm} = \frac{SR_{llm}}{SR_{llm} + SR_{vq}}$.
15: **end for**
```

previous states, assuming the task is MDP-based.
**SDIL**:A HIL approach with an unsupervised sub-goal learner, using only the skill discovery component while omitting skill optimality estimation, as our expert bot generates optimal demonstrations. Sub-goal selection is performed by: $\arg\max_i \quad \frac{1/D(z^i, z_t^{'})}{\sum_{i=1}^{K} 1/D(z^i, z_t^{'})}$, where $D$ is the Euclidean distance, $z_t^{'}$ is the continuous output vector of $\pi_H$, $z^i \in \mathcal{C}$. We use Gumbel-Softmax (Jang et al., 2016) to replace the argmax for differentiability.
**Thought Cloning (TC)**: A HIL approach with supervised sub-goal learner. TC consists of a thought generator $\pi_u(th_t|s_t, th_{t-1})$ (where $th_t$ equals to our $z_t$) and an action generator $\pi_l(a_t|s_t, th_t)$. We apply the LLM-generated sub-goal representations $z_t^{(ref)}$ as labels for supervised training of $\pi_u$.

We also evaluate two variants of SEAL: SEAL-L, which relies solely on the LLM-label-based high-level sub-goal encoder, and SEAL, which uses the dual-encoder design. SEAL-L is compared with TC to highlight the effectiveness of the low-level transition-augmented design, while SEAL demonstrates the superiority of the dual-encoder approach over SEAL-L.

## 5.2 Main Results

| Task | # Traj | BC | LISA | SDIL | TC | SEAL-L | SEAL |
|---|---|---|---|---|---|---|---|
| KeyDoor | 30 | 0.09±0.02 | 0.09±0.02 | 0.23±0.05 | 0.26±0.02 | 0.27±0.06 | **0.30±0.04** |
| | 100 | 0.50±0.06 | 0.53±0.05 | 0.45±0.04 | 0.50±0.03 | 0.52±0.02 | **0.56±0.03** |
| | 150 | 0.67±0.05 | 0.66±0.03 | 0.63±0.05 | 0.69±0.05 | 0.68±0.03 | **0.75±0.04** |
| | 200 | 0.74±0.02 | 0.69±0.04 | 0.70±0.04 | 0.70±0.02 | 0.76±0.04 | **0.82±0.04** |
| GridWorld | 200 | 0.26±0.04 | 0.24±0.03 | 0.43±0.04 | **0.44±0.03** | 0.39±0.04 | 0.29±0.03 |
| | 300 | 0.31±0.04 | 0.44±0.05 | 0.48±0.01 | 0.52±0.07 | **0.65±0.04** | 0.61±0.02 |
| | 400 | 0.48±0.04 | 0.53±0.03 | 0.62±0.04 | 0.62±0.04 | 0.83±0.02 | **0.85±0.02** |

Table 1: **Simulation Results:** Success rates (ranging from 0 to 1) for completing the tasks of *Key-Door* and *Grid-World* (3 Objects), averaged over 5 random seeds. Our SEAL approach outperforms others in most cases. The best-performing method is highlighted in **bold**.

We first evaluate SEAL in two compositional environments: *KeyDoor* and *Grid-World* with 3 objects. Their limited sub-goals facilitate high-level encoder learning in HIL settings. We use LLM *GPT-4o* (Islam & Moushi, 2024) to decompose full task instructions into sub-goals: LLM gives sub-goal count $K = 4$ for *KeyDoor* and $K = 6$ for *Grid-World.* These sub-goals label states in the expert dataset for supervised encoder training. For fair comparison, unsupervised baselines (LISA, SDIL) use the same sub-goal counts. Additional details are in the Appendix.

We train the models using randomly sampled expert demonstrations, with 30, 100, 150, and 200 samples for the *KeyDoor* environments, and 200, 300, and 400 samples for *Grid-World* with 3 objects. *Grid-World* is more complex environment, so additional expert data is collected. Task success rates are reported in Table 1. The results show in most cases, our SEAL either outperforms or is competitive with the other baselines.

**Does LLM help capture a better task hierarchy?** We observe both HIL baselines and our SEAL outperform non-hierarchical behavior cloning (BC) thanks to additional information learned from hierarchical sub-goal structures. LLM-label-based methods like TC and our SEAL show greater and more consistent leading, particularly as training samples increase and the gap between BC and HIL narrows due to exposure to more scenarios. Such advantage partly stems from the LLM labels more accurately capturing the task's ground-truth hierarchical structure. As shown in Fig. 2, both TC and SEAL achieve higher sub-goal identification accuracy, while unsupervised methods like SDIL may struggle to capture this structure, leading to irregular actions. Additionally, the high-level plans generated by LLMs help determine the appropriate sub-goal space size, eliminating the need to tune hyper-parameter $K$ (the number of sub-goals). As shown in Fig. 3, both overestimating and underestimating the sub-goal count lead to performance degradation in unsupervised methods like LISA and SDIL, whereas SEAL captures a sub-goal space closer to the ground truth.

| Sub-goals | # Traj | BC | LISA | SDIL | TC | SEAL-L | SEAL |
|---|---|---|---|---|---|---|---|
| Pick up the Key (KeyDoor) | 30 | 0.29±0.05 | 0.22±0.03 | 0.42±0.05 | 0.52±0.04 | 0.55±0.10 | **0.56±0.04** |
| | 100 | 0.78±0.04 | 0.77±0.06 | 0.65±0.02 | 0.67±0.02 | **0.82±0.05** | 0.80±0.02 |
| | 150 | 0.81±0.06 | 0.81±0.03 | 0.80±0.02 | 0.82±0.03 | 0.93±0.02 | **0.93±0.04** |
| | 200 | 0.87±0.01 | 0.88±0.03 | 0.83±0.03 | 0.86±0.01 | 0.97±0.02 | **0.98±0.01** |
| Pick up Object 1 (GridWorld) | 200 | 0.58±0.09 | 0.58±0.05 | 0.79±0.02 | 0.78±0.04 | **0.83±0.04** | 0.67±0.03 |
| | 300 | 0.64±0.06 | 0.71±0.07 | 0.75±0.02 | 0.85±0.03 | **0.90±0.04** | 0.85±0.04 |
| | 400 | 0.75±0.03 | 0.79±0.03 | 0.85±0.03 | 0.87±0.04 | 0.95±0.02 | **0.98±0.01** |
| Pick up Object 2 (GridWorld) | 200 | 0.39±0.09 | 0.36±0.06 | 0.56±0.04 | **0.64±0.05** | 0.61±0.04 | 0.50±0.05 |
| | 300 | 0.44±0.06 | 0.55±0.06 | 0.59±0.03 | 0.52±0.05 | **0.80±0.04** | 0.73±0.03 |
| | 400 | 0.57±0.05 | 0.63±0.04 | 0.70±0.04 | 0.62±0.03 | **0.90±0.02** | 0.89±0.01 |

Table 2: Success rates of sub-goals completion in both *KeyDoor* and *Grid-World*, averaged over 5 random seeds. For the *KeyDoor* environment, the sub-goal is to pick up the key, while for *Grid-World* with 3 objects, the sub-goals are to pick up object 1 and object 2.

**Does Transition-augmented low-level policy help ensure the success of sub-goal transitions?** Compared to Thought Cloning (TC), which also uses a single encoder relying solely on LLM labels for sub-goal learning, our SEAL-L with a transition-augmented low-level encoder shows a significantly higher sub-goal completion rate (as shown in Table 2). This indicates that the transition-augmented low-level policy helps select appropriate actions at critical intermediate states during sub-goal transitions, improving the transition success rate.

| Object Num | # Traj | BC | LISA | SDIL | TC | SEAL-L | SEAL |
|---|---|---|---|---|---|---|---|
| 3 | 300 | 0.31±0.04 | 0.44±0.05 | 0.48±0.01 | 0.52±0.07 | **0.65±0.04** | 0.61±0.02 |
| | 400 | 0.48±0.04 | 0.53±0.03 | 0.62±0.04 | 0.62±0.04 | 0.83±0.02 | **0.85±0.02** |
| 4 | 400 | 0.16±0.03 | 0.13±0.01 | 0.22±0.04 | 0.24±0.05 | 0.26±0.03 | **0.32±0.03** |
| | 500 | 0.39±0.04 | 0.36±0.04 | 0.40±0.01 | 0.39±0.03 | 0.49±0.03 | **0.51±0.03** |
| 5 | 500 | 0.09±0.02 | 0.11±0.04 | 0.11±0.02 | 0.23±0.06 | 0.25±0.05 | **0.42±0.03** |
| | 600 | 0.30±0.03 | 0.47±0.03 | 0.64±0.05 | 0.35±0.03 | 0.65±0.03 | **0.73±0.03** |

Table 3: Success rates on longer-range compositional tasks (*Grid-World*) with 3, 4 and 5 objects.

**Does Dual-encoder design help enhance the performance of SEAL?** Compared to SEAL-L, which relies solely on the LLM-label-based sub-goal encoder, SEAL with a dual-encoder design shows slightly higher success rates across both tasks. This advantage is more pronounced for longer compositional tasks with more sub-goals. As shown in Table 3, when we extend the *Grid-World* environment with more objects (4 and 5 objects, LLM-decomposed sub-goal numbers $K = 8, 10$ respectively), purely supervisory methods like TC and SEAL-L struggle due to the increasing difficulty of accurate sub-goal identification caused by sparsity of sub-goals. However, SEAL's dual-encoder design overcomes this issue by providing an unsupervised sub-goal learning alternative when the supervisory encoder becomes less effective.

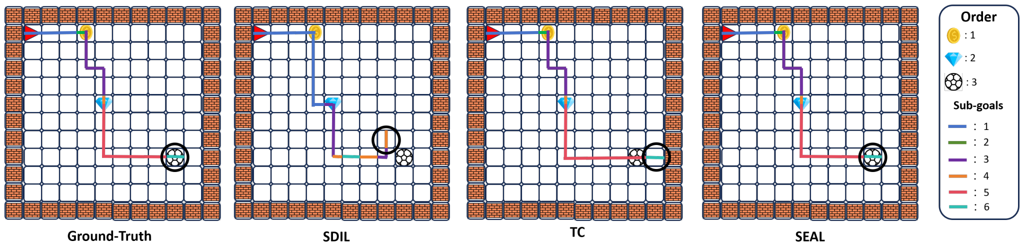

Figure 2: **Visualization:** Sub-goal selection in an example trajectory instance of *Grid-World* with 3 Objects. We color-code each sub-goal and black circle marks the final step of each trajectory. The ground-truth is labeled by human in this case, and SEAL achieve the best sub-goal transitions.

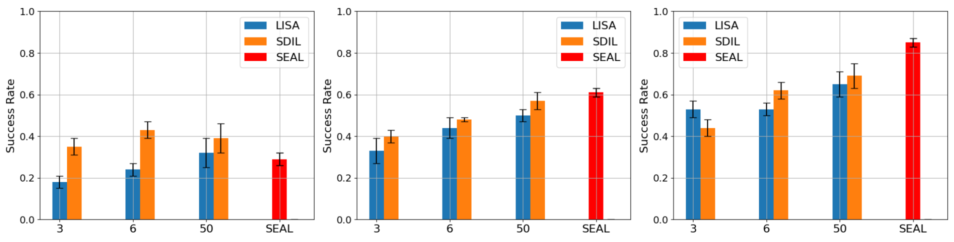

(a) #Traj = 200 (b) #Traj = 300 (c) #Traj = 400

Figure 3: Comparison of success rates among different sub-goal number $K$ selection in unsupervised HIL baselines LISA and SDIL. Experiments set on *Grid-World* with 3 Objects. $x$-axis represents the different settings of $K$.

## 5.3 Adaptation to Task Variations

To further evaluate SEAL's adaptability, we alter the pick-up order in the *Grid-World* environment (objects A, B, and C), creating new tasks. We use 400 expert demonstrations for the ABC order and 10 each for ACB, BCA, and BAC. The trained agent is then tested on these variations. As shown in Table 4, SEAL slightly outperforms baselines, suggesting better generalization. However, this only holds when order changes do not introduce new sub-goals so the learned sub-goals remain applicable, which indicates such adaptability of SEAL to task variations is limited.

Table 4: Success rates under task variations on *Grid-World* averaged over 5 random seeds.

| Test Env | BC | LISA | SDIL | TC | SEAL-L | SEAL |
|---|---|---|---|---|---|---|
| ABC | 0.48±0.04 | 0.53±0.03 | 0.62±0.04 | 0.62±0.04 | 0.83±0.02 | **0.85±0.02** |
| ACB | 0.01±0.00 | 0.08±0.02 | 0.11±0.04 | 0.13±0.05 | **0.18±0.07** | 0.14±0.03 |
| BAC | 0.01±0.00 | 0.05±0.01 | 0.06±0.02 | 0.09±0.02 | **0.11±0.03** | 0.08±0.02 |
| BCA | 0.00±0.00 | 0.03±0.01 | 0.08±0.03 | 0.08±0.02 | 0.08±0.01 | **0.09±0.03** |

## 6 Conclusion

In this work, we introduce SEAL, a novel HIL framework that leverages LLMs' semantic and world knowledge to define sub-goal spaces and pre-label states as meaningful sub-goal representations without prior task hierarchy knowledge. SEAL outperforms baselines like BC, LISA, SDIL, and TC, especially in low-sample and complex long-range compositional tasks, achieving higher success and sub-goal completion rates. The dual-encoder design proves more robust than the pure LLM encoder, and the transition-augmented low-level policy enhances sub-goal transitions. SEAL also adapts well to varying task complexities and latent dimensions. However, training instability remains a challenge, and we aim to make SEAL more standardized and efficient, particularly for tasks with partially observed states, more complex sub-goal space and more ambiguous textual instructions.

## 7 Ethics Statement

In this work, we develop a new algorithm for hierarchical imitation learning, which builds upon pretrained large language models (LLMs). The LLMs used in our experiments are based on publicly available GPT-4o API from OpenAI and do not involve any personally identifiable information or sensitive data. The authors are not aware of any additional ethical concerns related to the methodology presented in this research.

## References

Josh Achiam, Steven Adler, Sandhini Agarwal, Lama Ahmad, Ilge Akkaya, Florencia Leoni Aleman, Diogo Almeida, Janko Altenschmidt, Sam Altman, Shyamal Anadkat, et al. Gpt-4 technical report. *arXiv preprint arXiv:2303.08774*, 2023.

Michael Ahn, Anthony Brohan, Noah Brown, Yevgen Chebotar, Omar Cortes, Byron David, Chelsea Finn, Chuyuan Fu, Keerthana Gopalakrishnan, Karol Hausman, et al. Do as i can, not as i say: Grounding language in robotic affordances. *arXiv preprint arXiv:2204.01691*, 2022.

Arun Ahuja, Kavya Kopparapu, Rob Fergus, and Ishita Dasgupta. Hierarchical reinforcement learning with natural language subgoals. *arXiv preprint arXiv:2309.11564*, 2023.

Michael Bain and Claude Sammut. A framework for behavioural cloning. In *Machine Intelligence 15*, pp. 103–129, 1995.

Christopher Berner, Greg Brockman, Brooke Chan, Vicki Cheung, Przemyslaw Debiak, Christy Dennison, David Farhi, Quirin Fischer, Shariq Hashme, Chris Hesse, et al. Dota 2 with large scale deep reinforcement learning. *arXiv preprint arXiv:1912.06680*, 2019.

Kiante Brantley, Wen Sun, and Mikael Henaff. Disagreement-regularized imitation learning. In *International Conference on Learning Representations*, 2019.

Anthony Brohan, Yevgen Chebotar, Chelsea Finn, Karol Hausman, Alexander Herzog, Daniel Ho, Julian Ibarz, Alex Irpan, Eric Jang, Ryan Julian, et al. Do as i can, not as i say: Grounding language in robotic affordances. In *Conference on robot learning*, pp. 287–318. PMLR, 2023.

Sébastien Bubeck, Varun Chandrasekaran, Ronen Eldan, Johannes Gehrke, Eric Horvitz, Ece Kamar, Peter Lee, Yin Tat Lee, Yuanzhi Li, Scott Lundberg, et al. Sparks of artificial general intelligence: Early experiments with gpt-4. *arXiv preprint arXiv:2303.12712*, 2023.

Maxime Chevalier-Boisvert, Dzmitry Bahdanau, Salem Lahlou, Lucas Willems, Chitwan Saharia, Thien Huu Nguyen, and Yoshua Bengio. Babyai: A platform to study the sample efficiency of grounded language learning. *arXiv preprint arXiv:1810.08272*, 2018a.

Maxime Chevalier-Boisvert, Lucas Willems, and Suman Pal. Minimalistic gridworld environment for openai gym (2018). *URL https://github. com/maximecb/gym-minigrid*, 6, 2018b.

Yiming Ding, Carlos Florensa, Pieter Abbeel, and Mariano Phielipp. Goal-conditioned imitation learning. *Advances in neural information processing systems*, 32, 2019.

Yuqing Du, Olivia Watkins, Zihan Wang, Cédric Colas, Trevor Darrell, Pieter Abbeel, Abhishek Gupta, and Jacob Andreas. Guiding pretraining in reinforcement learning with large language models. In *International Conference on Machine Learning*, pp. 8657–8677. PMLR, 2023.

Eva Eigner and Thorsten Händler. Determinants of llm-assisted decision-making. *arXiv preprint arXiv:2402.17385*, 2024.

Yuwei Fu, Haichao Zhang, Di Wu, Wei Xu, and Benoit Boulet. Furl: Visual-language models as fuzzy rewards for reinforcement learning. *arXiv preprint arXiv:2406.00645*, 2024.

Divyansh Garg, Skanda Vaidyanath, Kuno Kim, Jiaming Song, and Stefano Ermon. Lisa: Learning interpretable skill abstractions from language. *Advances in Neural Information Processing Systems*, 35:21711–21724, 2022.

Milos Hauskrecht, Nicolas Meuleau, Leslie Pack Kaelbling, Thomas L Dean, and Craig Boutilier. Hierarchical solution of markov decision processes using macro-actions. *arXiv preprint arXiv:1301.7381*, 2013.

Joey Hejna, Pieter Abbeel, and Lerrel Pinto. Improving long-horizon imitation through instruction prediction. In *Proceedings of the AAAI Conference on Artificial Intelligence*, volume 37, pp. 7857–7865, 2023.

Jonathan Ho and Stefano Ermon. Generative adversarial imitation learning. *Advances in neural information processing systems*, 29, 2016.

Bin Hu, Chenyang Zhao, Pu Zhang, Zihao Zhou, Yuanhang Yang, Zenglin Xu, and Bin Liu. Enabling intelligent interactions between an agent and an llm: A reinforcement learning approach. *arXiv preprint arXiv:2306.03604*, 2023.

Shengran Hu and Jeff Clune. Thought cloning: Learning to think while acting by imitating human thinking. *Advances in Neural Information Processing Systems*, 36, 2024.

Wenlong Huang, Pieter Abbeel, Deepak Pathak, and Igor Mordatch. Language models as zero-shot planners: Extracting actionable knowledge for embodied agents. In *International conference on machine learning*, pp. 9118–9147. PMLR, 2022.

Wenlong Huang, Chen Wang, Ruohan Zhang, Yunzhu Li, Jiajun Wu, and Li Fei-Fei. Voxposer: Composable 3d value maps for robotic manipulation with language models. *arXiv preprint arXiv:2307.05973*, 2023.

Raisa Islam and Owana Marzia Moushi. Gpt-4o: The cutting-edge advancement in multimodal llm. *Authorea Preprints*, 2024.

Abhinav Jain and Vaibhav Unhelkar. Go-dice: Goal-conditioned option-aware offline imitation learning via stationary distribution correction estimation. In *Proceedings of the AAAI conference on artificial intelligence*, volume 38, pp. 12763–12772, 2024.

Eric Jang, Shixiang Gu, and Ben Poole. Categorical reparameterization with gumbel-softmax. *arXiv preprint arXiv:1611.01144*, 2016.

Yiding Jiang, Evan Liu, Benjamin Eysenbach, J Zico Kolter, and Chelsea Finn. Learning options via compression. *Advances in Neural Information Processing Systems*, 35:21184–21199, 2022.

Mingxuan Jing, Wenbing Huang, Fuchun Sun, Xiaojian Ma, Tao Kong, Chuang Gan, and Lei Li. Adversarial option-aware hierarchical imitation learning. In *International Conference on Machine Learning*, pp. 5097–5106. PMLR, 2021.

Zhaoxun Ju, Chao Yang, Fuchun Sun, Hongbo Wang, and Yu Qiao. Rethinking mutual information for language conditioned skill discovery on imitation learning. In *Proceedings of the International Conference on Automated Planning and Scheduling*, volume 34, pp. 301–309, 2024.

Dmitry Kalashnikov, Jacob Varley, Yevgen Chebotar, Benjamin Swanson, Rico Jonschkowski, Chelsea Finn, Sergey Levine, and Karol Hausman. Mt-opt: Continuous multi-task robotic reinforcement learning at scale. *arXiv preprint arXiv:2104.08212*, 2021.

Subbarao Kambhampati, Karthik Valmeekam, Lin Guan, Kaya Stechly, Mudit Verma, Siddhant Bhambri, Lucas Saldyt, and Anil Murthy. Llms can't plan, but can help planning in llm-modulo frameworks. *arXiv preprint arXiv:2402.01817*, 2024.

Junsu Kim, Younggyo Seo, and Jinwoo Shin. Landmark-guided subgoal generation in hierarchical reinforcement learning. *Advances in neural information processing systems*, 34:28336–28349, 2021.

Diederik P Kingma. Adam: A method for stochastic optimization. *arXiv preprint arXiv:1412.6980*, 2014.

Thomas Kipf, Yujia Li, Hanjun Dai, Vinicius Zambaldi, Alvaro Sanchez-Gonzalez, Edward Grefenstette, Pushmeet Kohli, and Peter Battaglia. Compile: Compositional imitation learning and execution. In *International Conference on Machine Learning*, pp. 3418–3428. PMLR, 2019.

Karol Kurach, Mario Lucic, Xiaohua Zhai, Marcin Michalski, and Sylvain Gelly. The gan landscape: Losses, architectures, regularization, and normalization. 2018.

Minae Kwon, Sang Michael Xie, Kalesha Bullard, and Dorsa Sadigh. Reward design with language models. *arXiv preprint arXiv:2303.00001*, 2023.

Hoang Le, Nan Jiang, Alekh Agarwal, Miroslav Dudík, Yisong Yue, and Hal Daumé III. Hierarchical imitation and reinforcement learning. In *International conference on machine learning*, pp. 2917–2926. PMLR, 2018a.

Lei Le, Andrew Patterson, and Martha White. Supervised autoencoders: Improving generalization performance with unsupervised regularizers. *Advances in neural information processing systems*, 31, 2018b.

Yang Liu, Yuanshun Yao, Jean-Francois Ton, Xiaoying Zhang, Ruocheng Guo, Hao Cheng, Yegor Klochkov, Muhammad Faaiz Taufiq, and Hang Li. Trustworthy llms: a survey and guideline for evaluating large language models' alignment. *arXiv preprint arXiv:2308.05374*, 2023.

Yecheng Jason Ma, William Liang, Guanzhi Wang, De-An Huang, Osbert Bastani, Dinesh Jayaraman, Yuke Zhu, Linxi Fan, and Anima Anandkumar. Eureka: Human-level reward design via coding large language models. *arXiv preprint arXiv:2310.12931*, 2023.

Federico Malato, Florian Leopold, Andrew Melnik, and Ville Hautamäki. Zero-shot imitation policy via search in demonstration dataset. In *ICASSP 2024-2024 IEEE International Conference on Acoustics, Speech and Signal Processing (ICASSP)*, pp. 7590–7594. IEEE, 2024.

Angelos Mavrogiannis, Christoforos Mavrogiannis, and Yiannis Aloimonos. Cook2ltl: Translating cooking recipes to ltl formulae using large language models. In *2024 IEEE International Conference on Robotics and Automation (ICRA)*, pp. 17679–17686. IEEE, 2024.

Oier Mees, Lukas Hermann, and Wolfram Burgard. What matters in language conditioned robotic imitation learning over unstructured data. *IEEE Robotics and Automation Letters*, 7(4):11205–11212, 2022.

Ofir Nachum, Shixiang Shane Gu, Honglak Lee, and Sergey Levine. Data-efficient hierarchical reinforcement learning. *Advances in neural information processing systems*, 31, 2018.

Suraj Nair and Chelsea Finn. Hierarchical foresight: Self-supervised learning of long-horizon tasks via visual subgoal generation. *arXiv preprint arXiv:1909.05829*, 2019.

Andrew Y Ng, Stuart Russell, et al. Algorithms for inverse reinforcement learning. In *Icml*, volume 1, pp. 2, 2000.

Xinlei Pan, Eshed Ohn-Bar, Nicholas Rhinehart, Yan Xu, Yilin Shen, and Kris M Kitani. Human-interactive subgoal supervision for efficient inverse reinforcement learning. *arXiv preprint arXiv:1806.08479*, 2018.

Bharat Prakash, Nicholas Waytowich, Tim Oates, and Tinoosh Mohsenin. Interactive hierarchical guidance using language. *arXiv preprint arXiv:2110.04649*, 2021.

Bharat Prakash, Tim Oates, and Tinoosh Mohsenin. Llm augmented hierarchical agents. *arXiv preprint arXiv:2311.05596*, 2023.

Marc'Aurelio Ranzato and Martin Szummer. Semi-supervised learning of compact document representations with deep networks. In *Proceedings of the 25th international conference on Machine learning*, pp. 792–799, 2008.

Siddharth Reddy, Anca D Dragan, and Sergey Levine. Sqil: Imitation learning via reinforcement learning with sparse rewards. *arXiv preprint arXiv:1905.11108*, 2019.

Stefan Schaal. Learning from demonstration. *Advances in neural information processing systems*, 9, 1996.

Tom Silver, Varun Hariprasad, Reece S Shuttleworth, Nishanth Kumar, Tomás Lozano-Pérez, and Leslie Pack Kaelbling. Pddl planning with pretrained large language models. In *NeurIPS 2022 foundation models for decision making workshop*, 2022.

Anthony Simeonov, Yilun Du, Beomjoon Kim, Francois Hogan, Joshua Tenenbaum, Pulkit Agrawal, and Alberto Rodriguez. A long horizon planning framework for manipulating rigid pointcloud objects. In *Conference on Robot Learning*, pp. 1582–1601. PMLR, 2021.

Ishika Singh, Valts Blukis, Arsalan Mousavian, Ankit Goyal, Danfei Xu, Jonathan Tremblay, Dieter Fox, Jesse Thomason, and Animesh Garg. Progprompt: Generating situated robot task plans using large language models. In *2023 IEEE International Conference on Robotics and Automation (ICRA)*, pp. 11523–11530. IEEE, 2023.

Chan Hee Song, Jiaman Wu, Clayton Washington, Brian M Sadler, Wei-Lun Chao, and Yu Su. Llm-planner: Few-shot grounded planning for embodied agents with large language models. In *Proceedings of the IEEE/CVF International Conference on Computer Vision*, pp. 2998–3009, 2023.

Simon Stepputtis, Joseph Campbell, Mariano Phielipp, Stefan Lee, Chitta Baral, and Heni Ben Amor. Language-conditioned imitation learning for robot manipulation tasks. *Advances in Neural Information Processing Systems*, 33:13139–13150, 2020.

Karthik Valmeekam, Matthew Marquez, Sarath Sreedharan, and Subbarao Kambhampati. On the planning abilities of large language models-a critical investigation. *Advances in Neural Information Processing Systems*, 36:75993–76005, 2023.

Aaron Van Den Oord, Oriol Vinyals, et al. Neural discrete representation learning. *Advances in neural information processing systems*, 30, 2017.

Xin Wang, Qiuyuan Huang, Asli Celikyilmaz, Jianfeng Gao, Dinghan Shen, Yuan-Fang Wang, William Yang Wang, and Lei Zhang. Reinforced cross-modal matching and self-supervised imitation learning for vision-language navigation. In *Proceedings of the IEEE/CVF conference on computer vision and pattern recognition*, pp. 6629–6638, 2019a.

Xin Wang, Shinji Takaki, Junichi Yamagishi, Simon King, and Keiichi Tokuda. A vector quantized variational autoencoder (vq-vae) autoregressive neural $f\_0$ model for statistical parametric speech synthesis. *IEEE/ACM Transactions on Audio, Speech, and Language Processing*, 28:157–170, 2019b.

Zihao Wang, Shaofei Cai, Guanzhou Chen, Anji Liu, Xiaojian Ma, and Yitao Liang. Describe, explain, plan and select: Interactive planning with large language models enables open-world multi-task agents. *arXiv preprint arXiv:2302.01560*, 2023.

Jason Wei, Xuezhi Wang, Dale Schuurmans, Maarten Bosma, Fei Xia, Ed Chi, Quoc V Le, Denny Zhou, et al. Chain-of-thought prompting elicits reasoning in large language models. *Advances in neural information processing systems*, 35:24824–24837, 2022.

Zheng Wen, Doina Precup, Morteza Ibrahimi, Andre Barreto, Benjamin Van Roy, and Satinder Singh. On efficiency in hierarchical reinforcement learning. *Advances in Neural Information Processing Systems*, 33:6708–6718, 2020.

Yaqi Xie, Chen Yu, Tongyao Zhu, Jinbin Bai, Ze Gong, and Harold Soh. Translating natural language to planning goals with large-language models. *arXiv preprint arXiv:2302.05128*, 2023.

Deheng Ye, Guibin Chen, Wen Zhang, Sheng Chen, Bo Yuan, Bo Liu, Jia Chen, Zhao Liu, Fuhao Qiu, Hongsheng Yu, et al. Towards playing full moba games with deep reinforcement learning. *Advances in Neural Information Processing Systems*, 33:621–632, 2020.

Yuexiang Zhai, Christina Baek, Zhengyuan Zhou, Jiantao Jiao, and Yi Ma. Computational benefits of intermediate rewards for goal-reaching policy learning. *Journal of Artificial Intelligence Research*, 73:847–896, 2022.

Alex Zhang, Ananya Parashar, and Dwaipayan Saha. A simple framework for intrinsic reward-shaping for rl using llm feedback.

Lihua Zhang. Sample efficient imitation learning via reward function trained in advance. *arXiv preprint arXiv:2111.11711*, 2021.

Yichi Zhang and Joyce Chai. Hierarchical task learning from language instructions with unified transformers and self-monitoring. *arXiv preprint arXiv:2106.03427*, 2021.

Tianxiang Zhao, Wenchao Yu, Suhang Wang, Lu Wang, Xiang Zhang, Yuncong Chen, Yanchi Liu, Wei Cheng, and Haifeng Chen. Skill disentanglement for imitation learning from suboptimal demonstrations. In *Proceedings of the 29th ACM SIGKDD Conference on Knowledge Discovery and Data Mining*, pp. 3513–3524, 2023.

## A Simulation Environmental Setup

**KeyDoor** The MiniGrid Dataset (Chevalier-Boisvert et al., 2018b) is a collection of grid-based environments designed for evaluating reinforcement learning and imitation learning algorithms in tasks requiring navigation, exploration, and planning. Among these environments, we start with *KeyDoor*, an easy-level compositional task that requires the player to move to the key and pick up it to unlock the door. To add complexity, we enlarge the original $3 \times 3$ grid environment to $10 \times 10$ size, and randomly initialize the locations of player, key and door for each episode. To facilitate understanding by LLMs, we convert the environment into a vector-based state, with elements including the coordinates of the player, key, and door, as well as the different statuses of the key (picked or not) and door (locked or not). The maximum time-steps $T$ of one episode is set to 100. We evaluate our SEAL on expert datasets with 30, 100, 150, 200 demonstrations generated by an expert bot.

**Grid-World** The environment is a 10x10 grid world with a single player and multiple objects randomly distributed at various locations. The player's objective is to visit and pick up these objects in a specific order. This task is more challenging than *KeyDoor* due to its longer-range compositional nature, involving more sub-goals. In this work, we set the number of objects in the grid world to range from 3 to 5, to test SEAL's effectiveness in solving longer-range tasks. Similar to *KeyDoor*, the fully observed environment is converted into a vector-based state, with elements representing the coordinates of the player and objects, as well as their statuses (picked or not). The maximum time-steps per episode is set to 100. We evaluate SEAL on expert datasets with 200, 300, and 400 demonstrations generated by an expert bot.

## B Additional Environment Information

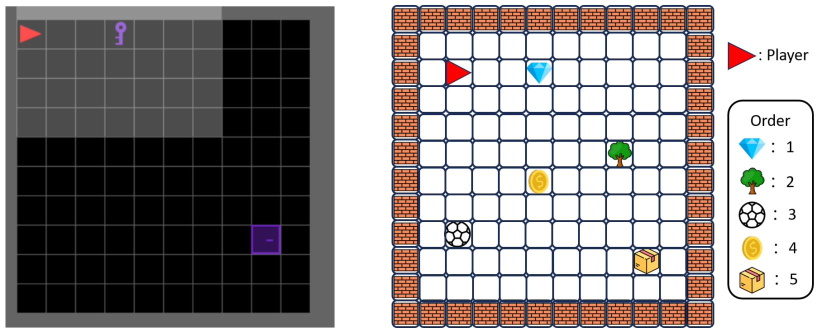

Figure 4: Examples of compositional-task-related environments used in our experiments. **Left:** *KeyDoor*. The player needs to pick up the key and then use it to unlock the door. **Right:** *Grid-World*. The player needs to pick up the different objects in a pre-specified order.

**KeyDoor** The environment is based on the *DoorKey* setting from the MiniGrid Dataset, but with modifications to make the state compatible with LLM input for sub-goal mapping. Instead of using image states, we convert the state into an 8-dimensional vector that captures crucial object information: {x-coordinate of key, y-coordinate of key, x-coordinate of door, y-coordinate of door, x-coordinate of player, y-coordinate of player, key status (picked: 1, not picked: 0), and door status (unlocked: 1, locked: 0) }. Wall obstacles are removed to avoid interference. The action space consists of 6 primitive actions: move up, move down, move right, move left, pick up, and unlock. The key can be picked up only when the player reaches the key's coordinates, and the door can be unlocked only if the player reaches the door's coordinates with the key already picked up. The language task instruction $\mathcal{M}$ is defined as: *"Pick up the key, and then unlock the door."* The episode ends when the door is successfully unlocked or the maximum time steps $T = 100$ are reached.

**Grid-World** The environment is based on the grid world used in (Kipf et al., 2019; Jiang et al., 2022). Similar to *KeyDoor*, the image-based states are converted into a vector format for LLM input, capturing crucial information about objects: x and y coordinates of Object 1, x and y coordinates of Object 2, ..., x and y coordinates of the player, status of Object 1 (picked: 1, not picked: 0), status of Object 2, .... For *Grid-World* with 3, 4, or 5 objects, the state vector has dimensions 11, 14, and

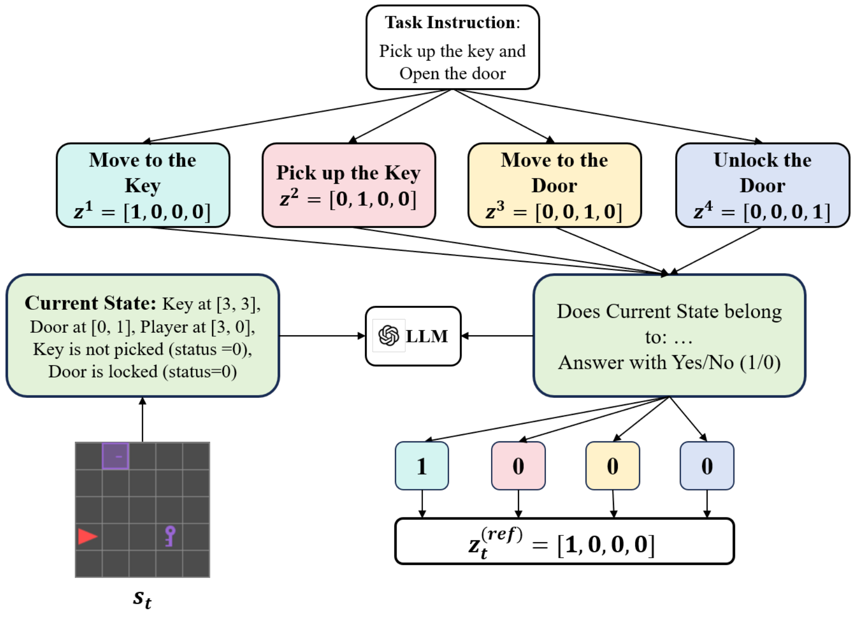
Task Instruction:
Pick up the key and Open the door
Move to the Key $z^1 = [1,0,0,0]$
Pick up the Key $z^2 = [0,1,0,0]$
Move to the Door $z^3 = [0,0,1,0]$
Unlock the Door $z^4 = [0,0,0,1]$
Current State: Key at [3, 3], Door at [0, 1], Player at [3, 0], Key is not picked (status =0), Door is locked (status=0)
LLM
Does Current State belong to: … Answer with Yes/No (1/0)
1
0
0
0
$z_t^{(ref)} = [1,0,0,0]$
$s_t$

Figure 5: A schematic illustrating how LLMs are prompted to define sub-goal spaces from task instructions and map states to sub-goal representations, serving as supervisory labels for training the high-level sub-goal encoder in SEAL.

17, respectively. Wall obstacles and irrelevant objects are removed to avoid interference. The action space consists of 5 primitive actions: move up, move down, move right, move left, and pick up. An object can be picked up only when the player reaches its coordinates. The language task instruction $\mathcal{M}$ is defined as: *"Pick up Object 1, then pick up Object 2, then..."* The episode ends when the player picks up all objects in the correct order or after the maximum time step $T = 100$. At the start of each episode, the coordinates of all objects and the player are randomly reset.

**Sub-goal Spaces Identified by LLMs** We use GPT-4o to decompose the language task instructions for both the *KeyDoor* and *Grid-World* environments into their respective sub-goal spaces. In the *KeyDoor* environment, there are $K = 4$ sub-goals: {move to the key, pick up the key, move to the door, unlock the door}. In the *Grid-World* environment, with 3, 4, and 5 objects, the number of sub-goals is $K = 6$, $K = 8$, and $K = 10$, respectively, including: {move to object 1, pick up object 1, move to object 2, pick up object 2, ...}. For both sub-goal spaces, we parameterize each language sub-goal in it by a K-dim one hot vector.

## C Example Prompts

In SEAL, we prompt LLMs to generate supervisory labels for training the high-level encoder. Fig. 5 illustrates the detailed prompting process. First, we prompt the LLMs to break down the task instruction into a finite set of sub-goals. Then, for each state, the LLM is prompted $K$ times to determine whether it corresponds to each of the decomposed sub-goals, mapping the states to sub-goal representations. Example prompts for both task decomposition and sub-goal labeling are provided in the following sub-sections.

### C.1 Prompts for Task Decomposition

An example prompt used in *Grid-World* experiment with 3 objects for task decomposition is listed below. We use GPT-4o to produce the answer.

**# Task Description**: Pick up the key, then Pick up the ball, and then pick up the diamond.

**# Environment Details**:

The environment is a 10×10 2D Grid-world.

Objects {Key, Ball, Diamond, Player} (Key, Ball, and Diamond's coordinates are fixed, The player can move)

Observation Space: {o1: The coordinate of the key
o2: The coordinate of the ball
o3: The coordinate of the diamond
o4: The coordinate of player itself
o5: The status of key (picked/not)
o6: The status of ball (picked/not)
o7: The status of diamond (picked/not)}

Action Space: {move up/right/left/down, pick up}

**# Role Instruction:**
You should give an abstract plan to solve the given task step-by-step. For each step in plan, you need to extract relevant features in observation space. You should answer in format:

{Step 1:. . . , Relevant Features:{o1,....} , Step 2:. . . , Relevant Features:{o1,....} . . . . . . Step N: ..., Relevant Features:{o1,....} }

The GPT-4o answer with:

Here is the abstract plan to solve the task step-by-step, with relevant features in the observation space for each step:

**Step 1: Move the player to the key's coordinate.**
Relevant Features: o1: The coordinate of the key. o4: The coordinate of the player.

**Step 2: Pick up the key.**
Relevant Features: o1: The coordinate of the key. o4: The coordinate of the player. o5: Status of the key (picked/not).

**Step 3: Move the player to the ball's coordinate.**
Relevant Features: o2: The coordinate of the ball. o4: The coordinate of the player. o5: Status of the key (picked/not).

**Step 4: Pick up the ball.**
Relevant Features: o2: The coordinate of the ball. o4: The coordinate of the player. o6: Status of the ball (picked/not).

**Step 5: Move the player to the diamond's coordinate.**
Relevant Features: o3: The coordinate of the diamond. o4: The coordinate of the player. o5: Status of the key (picked/not). o6: Status of the ball (picked/not).

**Step 6: Pick up the diamond.**
Relevant Features: o3: The coordinate of the diamond. o4: The coordinate of the player. o7: Status of the diamond (picked/not).

This step-by-step plan ensures that the player collects the objects in the specific required order: key, ball, and then diamond.

### C.2 PROMPTS FOR MAPPING STATES TO SUB-GOAL REPRESENTATIONS

An example prompt used in *KeyDoor* experiment for mapping states in expert demonstration to sub-goal representations is listed below. We use GPT-4o to produce the answer.

**# Environment:**
A 2D-grid World with a key and and a door in it. The grid world's size is 10 * 10. The coordinate in grid is written as [x, y] (x=0,1,2,3,4, y=0,1,2,3,4) Key at the coordinate: [3, 3]. Door at the coordinate: [0, 1]. Key is not picked up. (key state = 0) Door is locked. (door state = 0)
(Hint: You can only pick up the key when you at the key location, and can only unlock the door when you are at the door location and have already picked up the key).

**# Current State:**
The player is currently at [3, 0]. The key state = 0. The door state = 0. The next coordinate of player is at [3,3].

**# Sub-goal Judgement:**
You need to judge which stage the player in:
1. The player should move to the Key.
2. The player should pick up the Key.
3. The player should move to the Door.
4. The player should unlock the Door.
Please check whether the current state in the above stages in turn. For each judgement please answer with 1(Yes) or 0 (No).

You should finally answer with a 4-dimension vector format: [1/0, 1/0, 1/0, 1/0]

The GPT-4o response with:

The current state of the player is at [3, 0] and the next coordinate is [3, 3], which is the location of the key.

Here's the judgment for each state:

The player should move to the Key: 1 (The player is moving towards the key)
The player should pick up the Key: 0 (The player is not yet at the key location)
The player should move to the Door: 0 (The player has not picked up the key yet)
The player should unlock the Door: 0 (The player needs to pick up the key first)

So, the 4-dimension vector is: **[1, 0, 0, 0]**

## D MODEL IMPLEMENTATION DETAILS

| Methods | Loss | Hidden dim of MLPs | $\beta$ |
|---|---|---|---|
| BC | $\mathcal{L}_{BC} = \mathbb{E}_{(s_t,a_t)\in\mathcal{D}} - \log\pi(a_t\|s_t)$ | [128, 128] | / |
| LISA | $\mathcal{L}_{LISA} = \beta\mathcal{L}_H^{(vq)}(s_t) + \mathcal{L}_L(s_t, z_t^{(vq)})$ | [128, 128] | 0.4 |
| SDIL | $\mathcal{L}_{SDIL} = \mathbb{E}_{(s_t,a_t)\in\mathcal{D}}\mathbb{E}_{z_t\in\pi_H(z_t\|s_t)} - \log\pi_L(a_t\|z_t, s_t)$ | [128, 128] | / |
| TC | $\mathcal{L}_{TC} = \mathbb{E}_{(s_t,a_t,z_t)\in\mathcal{D}} - \log(\beta\pi_H(z_t\|z_{t-1}, s_t) + \pi_L(a_t\|s_t, z_t))$ | [128, 128] | 0.4 |
| SEAL | $\mathcal{L}_{SEAL} = W_{llm}(\mathcal{L}_H^{(llm)} + \mathcal{L}_L^{(llm)}) + W_{vq}(\mathcal{L}_H^{(vq)} + \mathcal{L}_L^{(vq)})$ | [128, 128] | 0.4 |

Table 5: Hyperparameters settings of Model Implementations.

We outline the model implementation details for all four baselines and SEAL in the *KeyDoor* and *Grid-World* environments. For non-hierarchical BC baselines, we use a two-layer Multi-layer Perceptron (MLP) as the trainable policy agent $\pi(a_t|s_t)$. In HIL approaches like LISA, SDIL, and TC, this same two-layer MLP is used for both the high-level sub-goal encoder $\pi_H(s_t)$ and the low-level policy agent $\pi_L(a_t|s_t, z_t)$. We use Adam (Kingma, 2014) as the optimizer for all models, with learning rates initialized at 5e-5 for *KeyDoor* and 5e-6 for *Grid-World*. To ensure fair comparison, we maintain consistent hyper-parameters across all simulations, including the high-level encoder loss weight $\beta$, the hidden dimensions of the MLPs, and the number of sub-goals $K$ for both HIL baselines and SEAL. Detailed implementations are presented in Table 5.